haematologica
Journal of the Ferrata Storti Foundation

Single-cell analysis unveils distinct transcriptional alterations and cellular origins in IgD multiple myeloma

by Tiancheng Luo, Xinyi Zhou, Xi Chen, Jin Liu, Ying Yang, Xiaoli Hu, Jing Li and Juan Du

Received: July 25, 2025.
Accepted: October 21, 2025.

Citation: Tiancheng Luo, Xinyi Zhou, Xi Chen, Jin Liu, Ying Yang, Xiaoli Hu, Jing Li and Juan Du. Single-cell analysis unveils distinct transcriptional alterations and cellular origins in IgD multiple myeloma. Haematologica. 2025 Oct 30. doi: 10.3324/haematol.2025.288418 [Epub ahead of print]

Single-cell analysis unveils distinct transcriptional alterations and cellular origins in IgD multiple myeloma

Tianchen Luo[1,†], Xinyi Zhou[1,†], Xi Chen[1,†], Jin Liu[1], Ying Yang[1], Xiaoli Hu[1], Jing Li[2,*], Juan Du[1,*]

Affiliations:

[1] Department of Hematology, Myeloma & Lymphoma Center, Shanghai Changzheng hospital; Shanghai, 200003, China.

[2] Center for Translational Medicine, Second Military Medical University (Naval Medical University); Shanghai, 200433, China.

[†] TCL, XYZ, and XC contributed equally to this article.

Corresponding author

Juan Du, M.D., Ph.D

Department of Hematology

Myeloma & Lymphoma Center

Shanghai Changzheng Hospital

Shanghai, China

Email: juan_du@live.com

and

Jing Li, M.D., Ph.D

Center for Translational Medicine

Naval Medical University

Shanghai, China.

Email: ljing@smmu.edu.cn

Conflict of interest statement: The authors declare no conflicts of interest.

Author Contributions

J.L. and J.D. designed the research and analyzed data. T.L., X.Z., X.C., Y.Y., and X.H performed research. J.L., Y.Y., X. H., and J.D. analyzed data. T.L., X.Z., T.L., X.Z., J.L. and J.D. wrote the paper.

Data avaliablity statement

The original scRNA-sequencing data sets generated in this study were deposited in the Genome Sequence Archive in the National Genomics Data Center, China National Center for Bioinformation, Chinese Academy of Sciences. The project accession number is PRJCA020281.

The code supporting the current study is available from the lead contact upon reasonable request.

Any additional information required to reanalyze the data reported in this

paper is available from the lead contact upon reasonable request.

Acknowledgements

This work was supported by the National Natural Science Foundation of China (82370206, 82170198), 2024 Shanghai Talents Plan, and the National Key R&D Program of China (2022YFA1305700).

Multiple myeloma (MM) is the second most prevalent blood cancer, distinguished by the secretion of monoclonal immunoglobulin, leading to organ dysfunction, anemia, renal impairment, and bone lesions(1). Despite remarkable advancements in therapeutic strategies, identifying and managing patients with poor outcomes under current regimens remains imperative. Immunoglobulin D (IgD) subtype, accounting for less than 2% of cases, exhibits inherently aggressive clinical traits: young age at presentation, higher incidence of extramedullary disease, osteolytic lesions, renal failure, etc(2). Despite advancements in response evaluation criteria, IgD myeloma continues to pose a significant survival challenge, with a median overall survival (OS) rate of approximately 3 years, notably lower than other subtypes(3, 4). To elucidate genetic alterations impacting IgD MM patient outcomes, we assembled 37 samples, comprising 13 IgD and 24 non-IgD MM samples. Bone marrow samples were obtained and used for sequencing. Samples were acquired with patients' written consent in accordance with the Declaration of Helsinki with approval from the Ethics Committee of Shanghai Changzheng Hospital (2016SL019A). 18 samples were sorted by CD138 microbeads, and the other 19 samples were not sorted. We conducted both single-cell RNA sequencing and single-cell B cell receptor sequencing analyses, and found significant differences in tumor cells between IgD MM and non-IgD MM, as well as notable microenvironmental changes. We processed and analyzed the gene expression matrix with the CellRanger

pipeline and the Seurat package. After low-quality cells were excluded, cell types were identified based on the high expression of marker genes. CNV alterations between IgD and non-IgD myeloma were identified using the InferCNV package. The Consensus Non-negative Matrix factorization (cNMF) was used to unravel the intratumoral expression profiles and meta-profiles of MM. Single-cell V(D)J data were processed with the Dandelion pipeline. Normal cells from unsorted samples were integrated with the Harmony package to remove batch effects and explore the difference between cells from various samples. Cell–cell interaction analysis was conducted using the LIANA package.

Firstly, we scrutinized the gene expression profiles and BCR features of tumor cells from both IgD MM and non-IgD MM. Each tumor predominantly harbored a main clone consistent with its clinical subtype (Supplemental Fig. 1). However, beyond the main clone, numerous subclones were identified, potentially diverging from clinical subtype identification, implying intra-tumor heterogeneity within patients. Given that MM arises from malignant plasma cells with a clonal B-cell origin, the emergence of sub-clones is generally uncommon. Through scVDJ analysis, we confirmed the clonal nature of tumor cells, observing a predominantly monoclonal pattern in all 18 sorted samples, as expected. Remarkably, we identified instances where cells exhibited identical VDJ regions but different immunoglobulin subtypes, suggesting the potential for antibody production post-tumor formation (Fig. 1A). We also

analyzed the preferences of constant and variable region transcription genes in BCRs across different groups, along with their physicochemical characteristics (Fig. 1B). Clustering of main clonal sequences translated into corresponding amino acid sequences from different samples revealed that in the heavy chain, the CDR3 length was predominantly concentrated in four lengths: 15, 17, 18, and 20 amino acids for VDJ motifs. Additionally, motif enrichment analysis indicated exclusion of IgG subtypes from group 1, while two out of three IgD subtypes and two out of six IgA subtypes were enriched in group 1 motifs. Group 4 motifs were exclusively associated with IgG subtypes, while four out of nine IgG subtypes were enriched in group 5. Regarding the light chain, the CDR3 length was predominantly concentrated in three lengths: 12, 13, and 15 for VJ motifs. One IgD sample did not match any motif, while the remaining two samples were all enriched in group 3 VJ motifs. Furthermore, four out of six IgA subtypes were enriched in group 2 motifs. These unveiled that the BCR of IgD MM appeared to possess more similar physicochemical properties compared to other BCR types. However, further investigation with an expanded sample size is warranted to explore this phenomenon comprehensively.

In addition, we identified higher rates of alterations in 1q+ in IgD myeloma through the inference of CNVs from single cell RNA-Seq expression data (Fig. 2). Among MM cases with 1q+, gain(1q) refers to those with only one extra copy of 1q, resulting in three total copies, while amp(1q) denotes patients

exhibiting amplification of 1q, characterized by the presence of two or more additional copies, totaling four or more copies(5). A recent systematic review of MM randomized controlled trials focusing on 1q+ found that patients with 1q+ compared to those without have poorer outcomes (6). Notably, 1q21 amplification was present in 76.9% (10/13) of IgD patients compared to 62.5% (15/24) of non-IgD patients (P = 0.47), potentially contributing to the poorer prognosis associated with this subtype.

Subsequently, we conducted a comparative analysis of the transcriptional features of MM through DEGs, cNMF-derived GEP, and enrichment analysis. Consistent with previous findings, we observed widespread involvement of ER stress and energy metabolism pathways in MM. DEGs in IgD MM and non-IgD MM were mainly enriched in protein processing and energy metabolism pathways. Aligning with our GEP analysis, we identified a total of 9 meta-programs associated with the disease, with the most significant one being metaprogram 2, consistently observed in all analyzed samples, covering gene signatures related to protein processing functions (Fig. 3A). However, upon examining the expression profiles of each sample in this meta-program, we found significant differences between IgD MM and non-IgD MM (Fig. 3B). Notably, ribosomal proteins (RPL19, RPL28, RPLP0, RPL18A, RPS4X, RPS5, RPL7A, RPLP1) within this signature may be associated with bortezomib response (7) (Fig. 3C). This may explain why our prior studies reported that IgD myeloma patients who received lenalidomide (an immunomodulatory drug,

IMiD) showed a better trend in median OS compared to patients who received bortezomib (a proteasome inhibitor, PI)(2), highlighting the importance of appropriate treatment selection for this IgD subgroup. Comparing differentially expressed genes, pathways related to ER stress, autophagy, and unfolded protein response were again enriched between malignant cells in IgD and non-IgD MM (Fig. 3D). Among the DEGs, the BCL-2 protein family serves as a core regulator in integrating stress signaling networks, regulating cell death, calcium homeostasis, the UPR and autophagy(8). Notably, we found higher expression of *BCL2*. Venetoclax, a BCL2-specific inhibitor, has shown promising results with higher response rates and longer progression-free survival for t(11;14) patients and those with high expression of BCL2(9). Thus, we speculate that IgD myeloma may be specifically sensitive to treatment regimens involving IMiD plus Venetoclax. Clinical research in this area needs further investigation.

The "seed and soil" hypothesis posits that the BME ("soil") may create a supportive survival niche for tumor cells ("seeds"). This microenvironment is comprised of a complex array of cells. In our investigation, we delved into the characteristics of the BME in IgD MM. We noted a distinct composition of B cells in the bone marrow of IgD MM patients (Supplemental Fig. 2A and 2B), with a higher proportion of immature B cells ($P = 0.014$). The ratios of B-cell populations in non-IgD samples mostly aligned with previous findings, with 3% pro-B cells, 8% pre-B cells, 7% immature B cells, and 83% mature B cells(10).

However, in IgD samples, the ratios were 12% pro-B cells, 40% pre-B cells, 21% immature B cells, and 27% mature B cells, indicating a higher proportion of immature B cells in IgD MM. Immature B cells in IgD MM displayed altered expression of genes characteristic of immature B cells such as BLK, BANK1, RAG2 (Supplemental Fig. 2C). BANK1 expression, which are integral to pathways crucial for B cell selection and function, such as BCR signaling and antigen processing and presentation via major histocompatibility complex (MHC) class II. The transient expression of pre-BCR and BCR signaling marks a critical checkpoint in B-cell development. Signals from the pre-BCR provide swift feedback regarding the functionality of the recombined Igμ gene, ensuring further maturation only for pre-B cells expressing a signaling-competent receptor(11). These findings suggest that IgD MM status may diminish BCR signaling, thereby curtailing survival and positive selection.

Furthermore, we conducted an extensive analysis of interactions among different cell types, with a particular focus on those between B cells and tumor cells. Several factors show significant differences between IgD MM and non-IgD MM in all unsorted samples (Supplemental Fig. 3A) as well as in newly diagnosed (ND) unsorted samples (Supplemental Fig. 3B). Factor 4 ($P < 0.05$) exhibited differences between the IgD and non-IgD groups for all unsorted samples and was primarily associated with myeloid cells, including pathways related to APP, GRN, CD23, MHC-I, and MHC-II (Supplemental Fig. 3C). CD23 played an essential role in B-cell responses and distinguishing various

immature and mature B-cell subsets(12). Remarkably, during the enrichment analysis of Factor 4-related pathways, we discovered that the expression of the TNFSF13B-related pathway was downregulated in IgD samples. TNFSF13B, also known as B cell-activating factor (BAFF), enhances B-cell survival and serves as a key regulator of the peripheral B-cell population. BAFFR is closely associated with BCR signaling. As we mentioned in the text, the distinct composition of B cells in the bone marrow of IgD MM patients may be related to diminished BCR signaling and antigen processing and presentation via the major histocompatibility complex (MHC) class II pathway, both of which are integral to pathways crucial for B cell selection and function. Similarly, for ND unsorted samples, Factor 4 ($P < 0.05$) presented differences between the IgD and non-IgD groups (Supplemental Fig. 3B). It was primarily linked to B cells and included pathways related to MIF, HMGB1, which played an essential role in B-cell responses and distinguishing various immature and mature B-cell subsets(12-18) (Supplemental Fig. 3D). The results further suggest that changes in B cell subtype proportions in IgD MM may be related to the impact of the BME. Also, the interaction between the tumor microenvironment and tumors varies by subtypes, contributing differently to tumor development.

In summary, we have characterized both common and distinct transcriptomic and clonal features of IgD MM compared to other MM subtypes at the single-cell resolution. We found IgD MM displayed a higher frequency of 1q21

amplification. Additionally, IgD MM revealed disparities in the endoplasmic reticulum stress pathway and higher BCL2 expression independent of t(11;14), suggesting its potential sensitivity to Venetoclax. IgD MM also exhibited notable microenvironmental changes, characterized by an increased presence of immature B cells, which may suggest a potential link to tumorigenesis. Furthermore, by analyzing motif patterns in VDJ/VJ, we found that the BCR of IgD MM tends to have a more similar clonotype with fewer subclones compared to non-IgD MM. While validation in larger cohorts and well-controlled randomized clinical trials is warranted, these findings illuminate the heterogeneity of MM and offer new perspectives for research and clinical treatment of IgD MM.

References

1. Siegel RL, Miller KD, Wagle NS, Jemal A. Cancer statistics, 2023. CA Cancer J Clin. 2023;73(1):17-48.
2. Liu J, Lu J, Qiang W, et al. Sensitive quantitative IgD assay increases progression-free survival prediction accuracy in IgD plasma cell myeloma. Leukemia. 2023;37(2):497-499.
3. Liu J, Hu X, Jia Y, et al. Clinical features and survival outcomes in IgD myeloma: a study by Asia Myeloma Network (AMN). Leukemia. 2021;35(6):1797-1802.
4. Lawless S, Sbianchi G, Morris C, et al. IgD subtype but not IgM or non-secretory is a prognostic marker for poor survival following autologous hematopoietic cell transplantation in multiple myeloma. Results from the EBMT CALM (collaboration to collect autologous transplant outcomes in lymphomas and myeloma) study. Clin Lymphoma Myeloma Leuk. 2021;21(10):686-693.
5. Schmidt TM, Fonseca R, Usmani SZ. Chromosome 1q21 abnormalities in multiple myeloma. Blood Cancer J. 2021;11(4):83.
6. Neupane K, Fortuna GG, Dahal R, et al. Alterations in chromosome 1q in multiple myeloma randomized clinical trials: a systematic review. Blood Cancer J. 2024;14(1):20.
7. Kang J, Brajanovski N, Chan KT, Xuan J, Pearson RB, Sanij E. Ribosomal proteins and human diseases: molecular mechanisms and targeted therapy. Signal Transduct Target Ther. 2021;6(1):323.
8. Pihán P, Carreras-Sureda A, Hetz C. BCL-2 family: integrating stress responses at the ER to control cell demise. Cell Death Diff. 2017;24(9):1478-1487.
9. Kumar SK, Harrison SJ, et al. Venetoclax or placebo in combination with bortezomib and dexamethasone in patients with relapsed or refractory multiple myeloma (BELLINI): a randomised, double-blind, multicentre, phase 3 trial. Lancet Oncol. 2020;21(12):1630-1642.
10. Tirier SM, Mallm JP, Steiger S, et al. Subclone-specific microenvironmental impact and drug response in refractory multiple myeloma revealed by single-cell transcriptomics. Nat Commun. 2021;12(1):6960.
11. Herzog S, Reth M, Jumaa H. Regulation of B-cell proliferation and differentiation by pre-B-cell receptor signalling. Nat Rev Immunol. 2009;9(3):195-205.
12. Cancro MP. Signalling crosstalk in B cells: managing worth and need. Nat Rev Immunol. 2009;9(9):657-661.
13. Garraud O, Borhis G, Badr G, et al. Revisiting the B-cell compartment in mouse and humans: more than one B-cell subset exists in the marginal zone and beyond. BMC Immunol. 2012;13:63.
14. Andreani V, Ramamoorthy S, Fässler R, Grosschedl R. Integrin β1 regulates marginal zone B cell differentiation and PI3K signaling. J Exp Med. 2023;220(1):e20220342.
15. Pelletier J, Balzano M, Destin J, et al. Niche-expressed Galectin-1 is involved in pre-B acute lymphoblastic leukemia relapse through pre-B cell receptor activation. iScience. 2023;26(4):106385.
16. Touarin P, Serrano B, Courbois A, et al. Pre-B cell receptor acts as a selectivity switch for galectin-1 at the pre-B cell surface. Cell Rep. 2024;43(8):114541.
17. Gore Y, Starlets D, Maharshak N, et al. Macrophage migration inhibitory factor induces B cell survival by activation of a CD74-CD44 receptor complex. J Biol Chem. 2008;283(5):2784-

2792.
18. Spagnuolo L, Puddinu V, Boss N, et al. HMGB1 promotes CXCL12-dependent egress of murine B cells from Peyer's patches in homeostasis. Eur J Immunol. 2021;51(8):1980-1991.

Figure legends

Fig. 1. Analysis of BCR profiles across 18 MM samples

(A) Comparison of different classes of myeloma malignant cells from patient S_IgG_RR_02, highlighting VDJ and VJ sequences with differing amino acids marked in red. Clones sharing the same VDJ and VJ but with different heavy chain C domains are boxed, offering insights into clonal evolution and diversity within individual patients.

(B) Motif analysis of VDJ and VJ sequences, with MM subtypes, new diagnoses, and relapses annotated on the right with metadata, providing insights into the sequence motifs associated with different MM subtypes and disease stages.

Fig. 2. CNVs of all samples

CNVs of all samples inferred by inferCNV. On the left, a summary of key information for all MM samples, including cytogenetic abnormalities detected by FISH. On the right, CNVs of all samples are depicted. Asterisk (*), cytogenetic abnormalities detected by FISH.

Fig. 3. Transcriptomic characteristics of IgD and non-IgD malignant plasma cells and experimental validation

(A) Pairwise correlation clustering of 115 gene expression profiles derived from cNMF analysis resulted in the formation of nine consensus modules. The biological significance of these modules was predicted through GO analysis.

(B) Comparison of the module score of M2 between IgD samples and non-IgD samples. Statistical significance is denoted by asterisks: *P < .05; **P < .01; ***P < .001, ****P < .0001.

(C) Expression profiles of M2 marker genes in IgD and non-IgD samples.

(D) GO enrichment analysis results for DEGs in malignant plasma cells (IgD vs. non-IgD).

(E) Differential gene expression analysis using the log-fold change expression versus the difference in the percentage of cells expressing the gene comparing IgD and non-IgD MM in ND patients (Δ Percentage Difference). The top 10 upregulated and downregulated genes, as well as some genes related to protein processing, were labeled.

Fig. 1

A

VDJ Junction			VJ Junction
CAKDQEVRTLRGGGFDYW	IgG	1	CQSADSSGTYGVF
CAP I FYGSGTYFPYW	IgG	1	CGTWDSSLRAGVF
CAPVFFGSGTYFPYW	IgG	1	CGTWDSSLRAGVF
CAPVFYGSGTYCPYW	IgG	1	CGTWDSSLRAGVF
CAPVFYGSGTYFPFW	IgG	1	CGTWDSSLRAGVF
CAPVFYGSGTYFPYS	IgG	1	CGTWDSSLRAGVF
CAPVFYGSGTYFPYW	IgD	3	CGTWDSSLRAGVF
CAPVFYGSGTYFPYW	IgG	9123	CGTWDSSLRAGVF
CAPVFYGSGTYFPYW	IgM	97	CGTWDSSLRAGVF
CATQGWQ-G -YFDVW	IgG	1	CQQYYNTPFTF

B

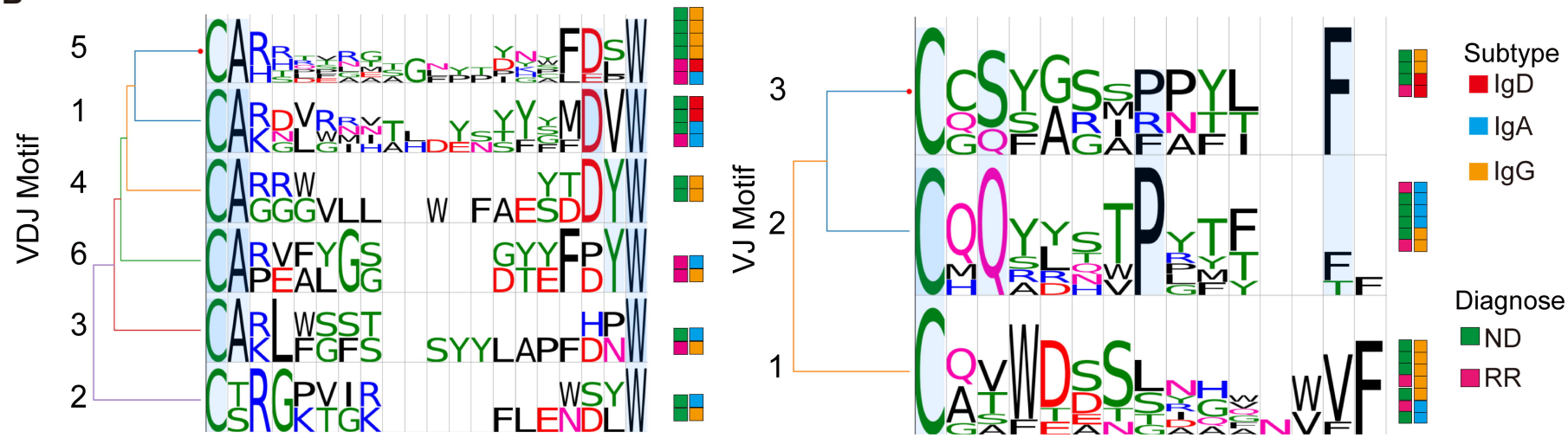

Fig. 2

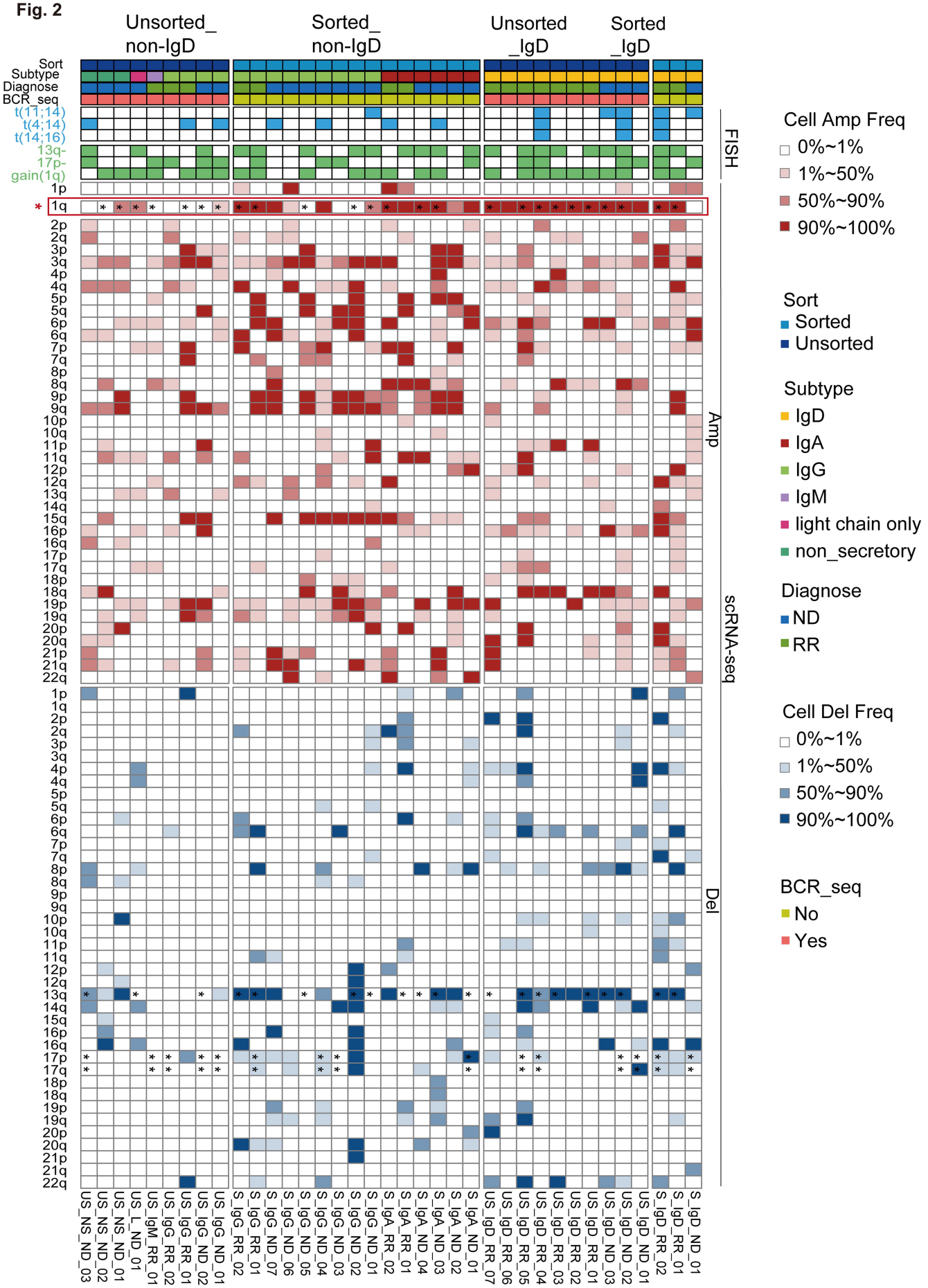
Unsorted_ non-IgD
Sorted_ non-IgD
Unsorted _IgD
Sorted _IgD
Sort
Subtype
Diagnose
BCR_seq
t(11;14)
t(4;14)
t(14;16)
13q-
17p-
gain(1q)
FISH
scRNA-seq
Amp
Del
1p
1q
2p
2q
3p
3q
4p
4q
5p
5q
6p
6q
7p
7q
8p
8q
9p
9q
10p
10q
11p
11q
12p
12q
13q
14q
15q
16p
16q
17p
17q
18p
18q
19p
19q
20p
20q
21p
21q
22q
US_NS_ND_03
US_NS_ND_02
US_NS_ND_01
US_L_ND_01
US_IgM_RR_01
US_IgG_RR_02
US_IgG_RR_01
US_IgG_ND_02
US_IgG_ND_01
S_IgG_RR_02
S_IgG_RR_01
S_IgG_ND_07
S_IgG_ND_06
S_IgG_ND_05
S_IgG_ND_04
S_IgG_ND_03
S_IgG_ND_02
S_IgG_ND_01
S_IgA_RR_02
S_IgA_RR_01
S_IgA_ND_04
S_IgA_ND_03
S_IgA_ND_02
S_IgA_ND_01
US_IgD_RR_07
US_IgD_RR_06
US_IgD_RR_05
US_IgD_RR_04
US_IgD_RR_03
US_IgD_RR_02
US_IgD_RR_01
US_IgD_ND_03
US_IgD_ND_02
US_IgD_ND_01
S_IgD_RR_02
S_IgD_RR_01
S_IgD_ND_01
Cell Amp Freq
0%~1%
1%~50%
50%~90%
90%~100%
Sort
Sorted
Unsorted
Subtype
IgD
IgA
IgG
IgM
light chain only
non_secretory
Diagnose
ND
RR
Cell Del Freq
0%~1%
1%~50%
50%~90%
90%~100%
BCR_seq
No
Yes

Fig. 3

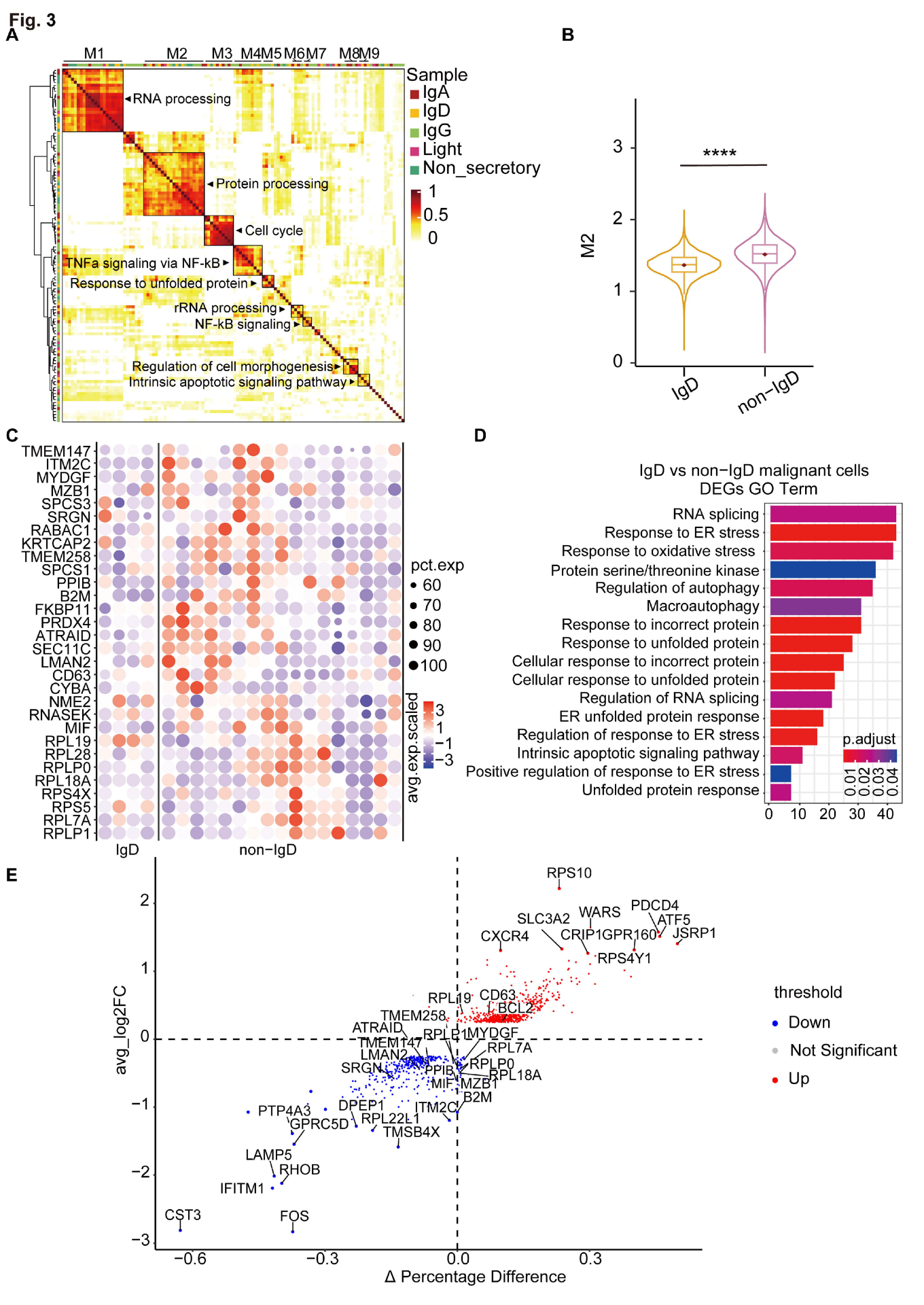
A
M1
M2
M3
M4M5
M6M7
M8M9
RNA processing
Protein processing
Cell cycle
TNFa signaling via NF-kB
Response to unfolded protein
rRNA processing
NF-kB signaling
Regulation of cell morphogenesis
Intrinsic apoptotic signaling pathway
Sample
IgA
IgD
IgG
Light
Non_secretory
1
0.5
0
B
****
M2
3
2
1
0
IgD
non−IgD
C
TMEM147
ITM2C
MYDGF
MZB1
SPCS3
SRGN
RABAC1
KRTCAP2
TMEM258
SPCS1
PPIB
B2M
FKBP11
PRDX4
ATRAID
SEC11C
LMAN2
CD63
CYBA
NME2
RNASEK
MIF
RPL19
RPL28
RPLP0
RPL18A
RPS4X
RPS5
RPL7A
RPLP1
IgD
non−IgD
pct.exp
60
70
80
90
100
avg.exp.scaled
3
1
−1
−3
D
IgD vs non−IgD malignant cells
DEGs GO Term
RNA splicing
Response to ER stress
Response to oxidative stress
Protein serine/threonine kinase
Regulation of autophagy
Macroautophagy
Response to incorrect protein
Response to unfolded protein
Cellular response to incorrect protein
Cellular response to unfolded protein
Regulation of RNA splicing
ER unfolded protein response
Regulation of response to ER stress
Intrinsic apoptotic signaling pathway
Positive regulation of response to ER stress
Unfolded protein response
p.adjust
0.01
0.02
0.03
0.04
0
10
20
30
40
E
RPS10
SLC3A2
WARS
PDCD4
ATF5
CXCR4
CRIP1
GPR160
JSRP1
RPS4Y1
RPL19
CD63
BCL2
TMEM258
ATRAID
RPLP1
MYDGF
TMEM147
RPL7A
LMAN2
RPLP0
SRGN
PPIB
RPL18A
MIF
MZB1
B2M
PTP4A3
DPEP1
ITM2C
GPRC5D
RPL22L1
TMSB4X
LAMP5
RHOB
IFITM1
CST3
FOS
avg_log2FC
2
1
0
−1
−2
−3
−0.6
−0.3
0.0
0.3
Δ Percentage Difference
threshold
Down
Not Significant
Up

Single-cell analysis unveils distinct transcriptional alterations and cellular origins in IgD multiple myeloma

Supplemental Figures

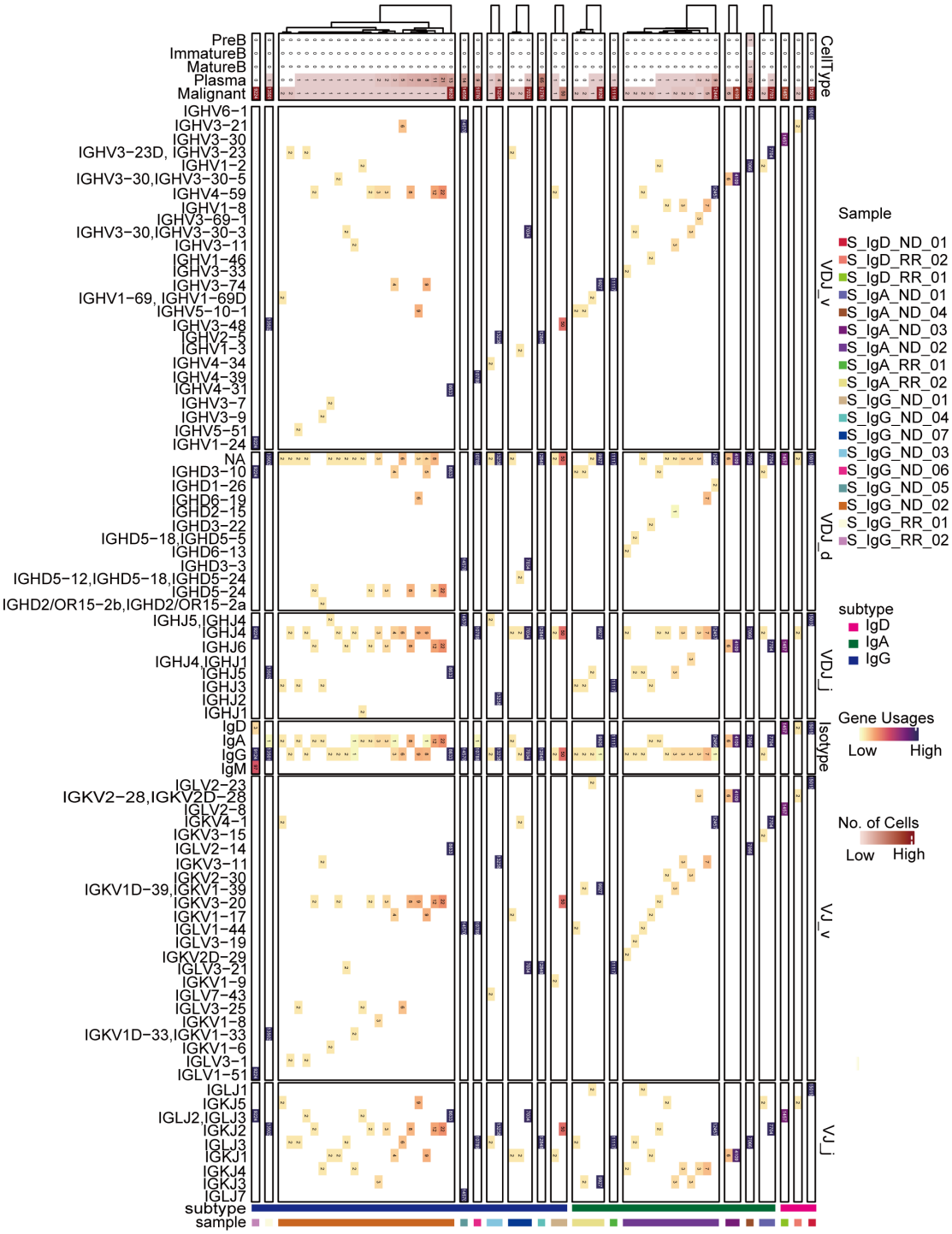

Supplemental Fig. 1. Single-cell BCR repertoire landscape of MM in sorted samples

In the top panel, cell numbers for each patient are plotted. The middle panel displays VDJ and VJ usage, isotypes, and cell numbers in a heatmap format, with MM subtypes labeled at the bottom, providing insights into the BCR profiles across different MM samples.

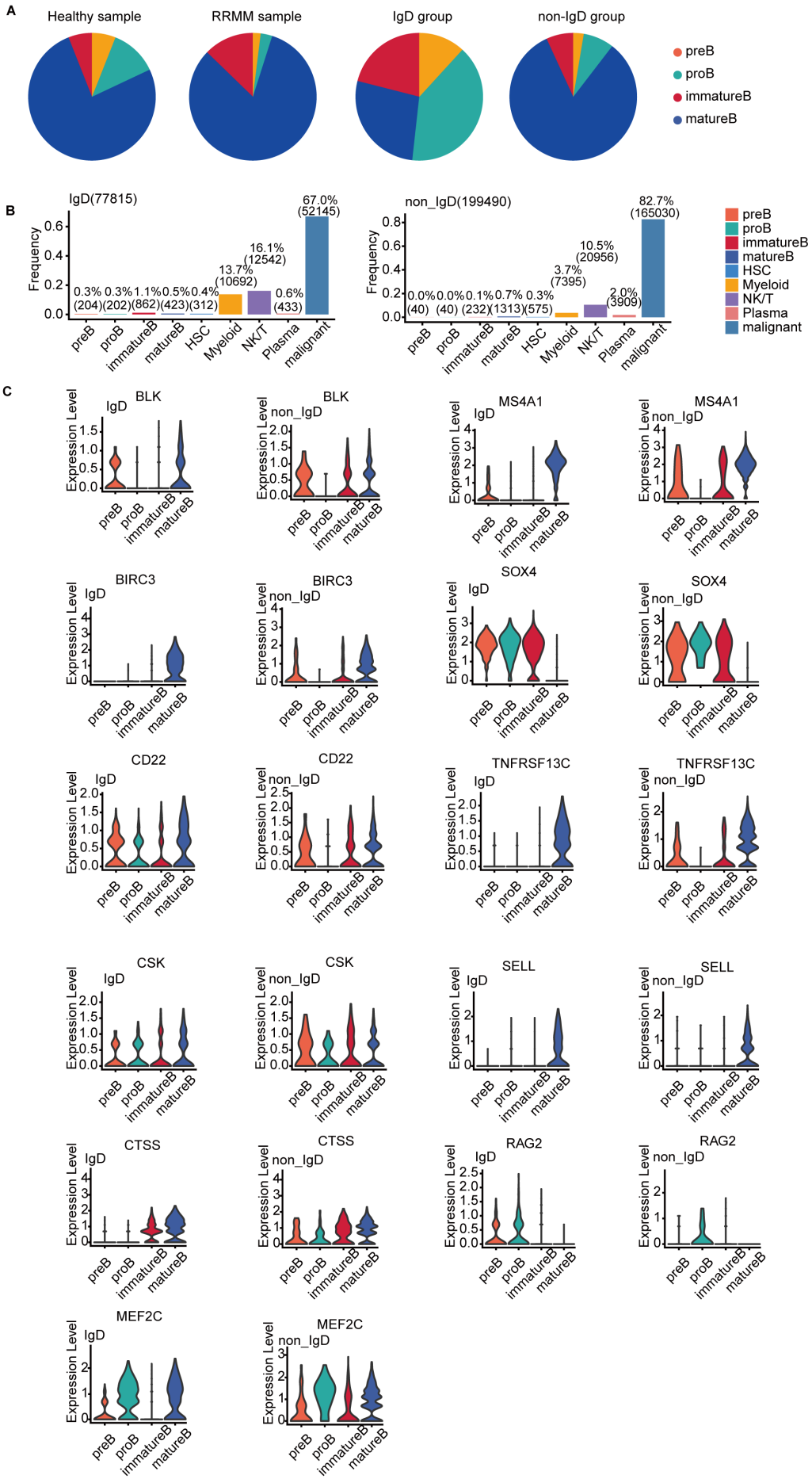
A
Healthy sample
RRMM sample
IgD group
non-IgD group
preB
proB
immatureB
matureB
B
IgD(77815)
Frequency
0.3% (204)
0.3% (202)
1.1% (862)
0.5% (423)
0.4% (312)
13.7% (10692)
16.1% (12542)
0.6% (433)
67.0% (52145)
non_IgD(199490)
0.0% (40)
0.0% (40)
0.1% (232)
0.7% (1313)
0.3% (575)
3.7% (7395)
10.5% (20956)
2.0% (3909)
82.7% (165030)
preB
proB
immatureB
matureB
HSC
Myeloid
NK/T
Plasma
malignant
C
BLK
MS4A1
BIRC3
SOX4
CD22
TNFRSF13C
CSK
SELL
CTSS
RAG2
MEF2C
IgD
non_IgD
Expression Level

Supplemental Fig. 2. Comparison of cell proportions and genes in the B cell receptor (BCR) signaling pathway

(A) Comparison of B cell type fractions between healthy donors and patients with RRMM (adapted from https://doi.org/10.1038/s41467-021-26951-z), IgD MM, and non-IgD MM (from this study).
(B) Bar plot illustrating the proportions of various cell types (IgD MM vs. non-IgD MM)
(C) Violin plot depicting the expression levels of differentially expressed genes in immature B cells comparing IgD and non-IgD multiple myeloma (MM), with a focus on the BCR signaling pathway. Genes such as MEF2C, BLK, MS4A1, BIRC3, SOX4, CD22, TNFRSF13C, CSK, SELL, CTSS, and RAG2 are highlighted for comparison between IgD MM and non-IgD MM

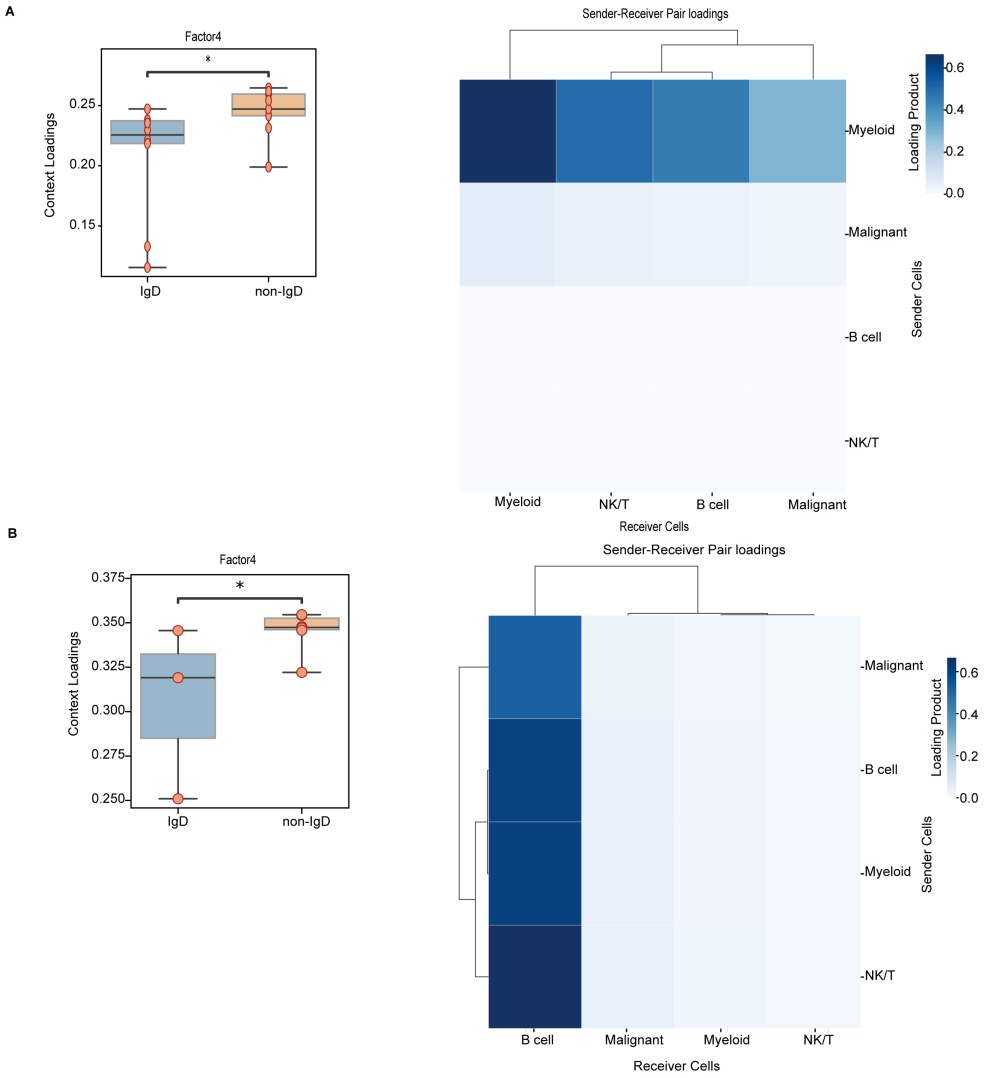
A
Factor4
Context Loadings
IgD
non-IgD
Sender-Receiver Pair loadings
Loading Product
Sender Cells
Myeloid
Malignant
B cell
NK/T
Receiver Cells
B
Factor4
Context Loadings
IgD
non-IgD
Sender-Receiver Pair loadings
Loading Product
Sender Cells
Malignant
B cell
Myeloid
NK/T
Receiver Cells
C
Factor1
Factor2
Factor3
Factor4
Loadings
D
Factor1
Factor2
Factor3
Factor4
Factor5
Factor6
Loadings

Supplemental Fig. 3. Analysis of communication patterns between IgD and non-IgD MM from the LIANA and Tensor-cell2cell framework (all unsorted samples and ND unsorted samples).

(A) Left, sample loadings were statistically compared between IgD MM and non-IgD MM within the same cell-cell communication program for all unsorted samples. Right, the heatmap illustrates the cell type loadings for Factor 4 for all unsorted samples.
(B) Left, sample loadings were statistically compared between IgD MM and non-IgD MM within the same cell-cell communication program for ND unsorted samples. Right, the heatmap illustrates the cell type loadings for Factor 4 for ND unsorted samples.
(C) The heatmap displays the ligand-receptor interactions loadings across all programs for all unsorted samples.
(D) The heatmap displays the ligand-receptor interactions loadings across all programs for ND unsorted samples.